Inorg. Chem. **2007**, *46*, 11165–11172

Dinuclear and Tetranuclear Gold–Nitrogen Complexes. Solvent Influences on Oxidation and Nuclearity of Gold Guanidinate Derivatives

Ahmed A. Mohamed,[†] Andrew P. Mayer,[†] Hanan E. Abdou,[†] Michael D. Irwin,[†] Lisa M. Pérez,[‡] and John P. Fackler, Jr.*[,†]

Laboratory for Molecular Structure and Bonding, Department of Chemistry, Texas A&M University, College Station, Texas 77843-3255, and Laboratory for Molecular Simulation, Texas A&M University, College Station, Texas 77843-3255

Received July 13, 2007

The sodium salt of the Hhpp ligand, Hhpp = 1,3,4,6,7,8-hexahydro-2*H*-pyrimido[1,2-*a*]pyrimidine, a 6,6 bicyclic, guanidine system, reacts with (THT)AuCl (THT = tetrahydrothiophene) in THF or CH_2Cl_2 to form the Au(II) complex, $[Au_2(hpp)_2Cl_2]$. The Au(II) complex forms either by oxidation with solvents such as CH_2Cl_2 or disproportionation of Au(I) with concomitant Au(0) formation. The reaction in ethanol gives the colorless tetranuclear Au(I) complex, $[Au_4(hpp)_4]$. The tbo ligand, Htbo = 1,4,6-triazabicyclo[3.3.0]oct-4-ene a bicyclic 5,5 guanidine system, behaved differently from the hpp ligand, and only the colorless tetranuclear gold complex, $[Au_4(tbo)_4]$, formed in THF, CH_2Cl_2, or ethanol. The X-ray structure of the oxidized species, $[Au_2(hpp)_2Cl_2]$, shows a Au(II)–Au(II) distance of 2.4752(9) Å, the shortest gold–gold bond reported prior to the characterization here of the $[(PhCOO)_6Au_4(hpp)_2Ag_2]$, Au(II)–Au(II) = 2.4473(19) Å. A preliminary description of the formation of this material, obtained by reacting $[Au_2(hpp)_2Cl_2]$ with Ag(OOCPh), is included in this paper. The four Au(I) atoms in the tetranuclear complexes are arranged in a parallelogram with Au–Au distances ranging from 2.8975(5)–2.9392(6) Å in $[Au_4(hpp)_4]$ and 3.1139(12)–3.2220(13) Å in $[Au_4(tbo)_4]$. density functional theory (DFT) and MP2 calculations on $[Au_2(hpp)_2Cl_2]$ find that the highest occupied molecular orbital (HOMO) is predominately hpp and chlorine-based with some Au–Au δ^* character. The lowest unoccupied molecular orbital (LUMO) has metal-to-ligand (M–L) and metal-to-metal (M–M) σ^* character (approximately 50% hpp/chlorine, and 50% gold). DFT calculations on $[Au_4(hpp)_4]$ show that the HOMO and HOMO-1 are each a mixture of metal–metal antibonding character and metal–ligand antibonding character and that the LUMO is predominately metal based s character (85% Au and 15% hpp).

Introduction

The chemistry of gold has grown rapidly in recent years, and along with this an improved understanding of gold–nitrogen bonding.[1] Relatively few compounds are known with Au(I)–N coordination to sp^2 N as found in pyridine[2] and related species such as the trinuclear pyrazolates[3] which dominate this chemistry. A few years ago, our laboratory started to examine carefully the chemistry of bidentate sp^2 N ligands bonded to Au(I) which were capable of bringing two Au(I) into close proximity. Previous studies with 1,1-dithiolates and ylides had demonstrated that a Au(II)–Au(II) bond could be formed upon oxidation, a chemistry unknown previously with nitrogen ligands.[4]

* Author to whom correspondence should be addressed. E-mail: fackler@mail.chem.tamu.edu.
[†] Department of Chemistry.
[‡] Laboratory for Molecular Simulation.

(1) Schmidbaur, H., Ed. *Gold: Progress in Chemistry, Biochemistry and Technology*; John Wiley & Sons: Chichester, U.K., 1999.
(2) (a) Conzelmann, W.; Hiller, W.; Strähle, J.; Sheldrick, G. M. *Z. Anorg. Allg. Chemie*. **1984**, *512*, 169–176. (b) Adams, H. N.; Hiller, W.; Strähle, J. *Z. Anorg. Allg. Chemie*. **1982**, *485*, 81–91. (c) Jutzi, P.; Heusler, H. *J. Organomet. Chem.* **1976**, *114*, 265–272.
(3) (a) Minghetti, G.; Banditelli, G.; Bonati, F. *Inorg. Chem.* **1979**, *18*, 658–663. (b) Raptis, R. G.; Murray, H. H., III; Fackler, J. P., Jr. *J. Chem. Soc., Chem. Commun*. **1987**, 737–739. (c) Raptis, R. G.; Murray, H. H.; Fackler, J. P., Jr. *Acta Crystallogr., Sect. C: Cryst. Struct. Commun.* **1988**, *C44*, 970–973. (d) Raptis, R. G.; Fackler, J. P., Jr. *Inorg. Chem.* **1988**, *27*, 4179–4182. (e) Barbera, J.; Elduque, A.; Gimenez, R.; Oro, L. A.; Serrano, J. L. *Angew. Chem., Int. Ed. Engl.* **1996**, *35*, 2832–2835. (f) Barbera, J.; Elduque, A.; Gimenez, R.; Lahoz, F. J.; Lopez, J. A.; Oro, L. A.; Serrano, J. L. *Inorg. Chem.* **1998**, *37*, 2960–2967. (g) Kim, S. J.; Kang, S. H.; Park, K.-M.; Kim, H.; Zin, W.-C.; Choi, M.-G.; Kim, K. *Chem. Mater*. **1998**, *10*, 1889–1893. (h) Yang, G.; Raptis, R. G. *Inorg. Chem*. **2003**, *42*, 261–263. (i) Yang, G.; Raptis, R. G. *Inorg. Chimica Acta* **2003**, *352*, 98–104. (j) Burini, A.; Mohamed, A. A.; Fackler, J. P. *Comments Inorg. Chem.* **2003**, *24*, 253–280. (k) Dodge, M. W.; Wacholtz, W. F.; Mague, J. T. *J. Chem. Crystallogr*. **2005**, *35*, 5–12.

10.1021/ic701399s CCC: $37.00
Published on Web 11/20/2007

Chart 1. Structures of the Anionic, Bidentate Nitrogen Ligands Discussed in This Paper

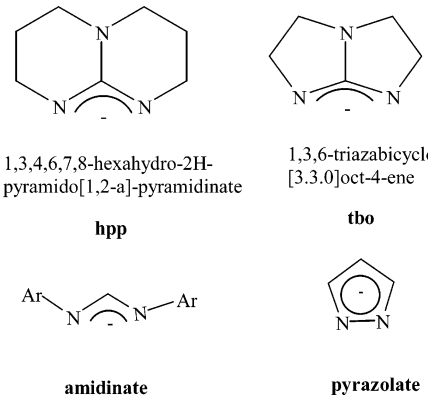

With amidinate nitrogen ligands, Chart 1, our laboratory has successfully synthesized several tetranuclear Au(I) species, most notably $[Au_4(ArNC(H)NAr)_4]$, where Ar = C_6H_4-4-OMe, C_6H_3-3,5-Cl, C_6H_4-4-Me.[5] Many of these gold cluster compounds, as well as the ones presented in this article, have been found to be excellent precursor catalysts for the oxidation of CO to CO_2 by gold nanoclusters on TiO_2 or MgO surfaces.[6] The formamidinate ligands are somewhat flexible around the N−C−N bond and can form products with various arrangements.[7]

The guanidinate-like ligand, used in the compounds described in this article, is unable to rotate around the N−C−N bond. Work with the anionic hpp ligand was pioneered by Cotton and co-workers who showed that the di-metal complexes with Cr(II), Mo(II), or W(II), ionize more readily than cesium.[8] Recent work with the hpp ligand in our laboratory has produced the compound $Au_2(hpp)_2Cl_2$, which we communicated to have the shortest Au−Au (2.47 Å) distance reported to date.[9] We also have reported recently[10] that amidinate complexes with bulky substitutents which prevent formation of tetrameric products form dinuclear Au(I) species which can be oxidized to metal−metal bonded Au(II) products.

Although it is known that the direction of the lone pairs of electrons on nitrogen ligands can influence the nuclearity of the complexes formed, as for example, with the 3,5-diphenylpyrazolate ligand which normally forms trinuclear complexes with Au(I) or Ag(I), Raptis and co-workers[3i] were able to obtain a tetranuclear Au(I) pyrazolate complex by using bulky groups at the 3 and 5 positions of the ring.

While we have been unsuccessful with many attempts by direct synthesis or reduction to isolate the Au(I) product $[Au_2(hpp)_2]$, we have discovered that solvent conditions determine whether oxidation to the dinuclear Au(II) species, $[Au_2(hpp)_2Cl_2]$, occurs or a tetranuclear Au(I) species, $[Au_4(hpp)_4]$, forms. It appears that the nuclearity of hpp compounds depends upon the solvent used and not upon steric effects, which, with bulky amidinate ligands,[10] are known to block the formation of tetranuclear complexes.

In order to examine why oxidation of a putative dinuclear Au(I) hpp complex occurs so readily, and to understand the factors influencing the stability of these and related amidinate complexes, DFT and MP2 calculations were conducted which suggest that both geometric factors and ligand π-bonding with the Au(I) influence the products produced.

Experimental Section

General Methods. All syntheses were performed under a nitrogen atmosphere, and all glassware was oven-dried prior to use. THF, CH_2Cl_2, ethanol, Hhpp, and Bu_4NPF_6 were purchased from Aldrich. The solvent, THF, was dried over Na/K alloy and CH_2Cl_2 over P_2O_5. All solvents, except ethanol, were freshly distilled under nitrogen prior to use. The H-tbo ligand was a generous gift from the Cotton Laboratory. UV−vis spectra were recorded on a Shimadzu UV-2501 PC spectrometer. ^{1}H spectra were recorded on a Unity Plus 300 NMR spectrometer using the $CHCl_3$ in the solvent peak to reference the chemical shifts (δ). Emission and excitation spectra were recorded on a SLM AMINCO Model 8100 spectrofluorometer equipped with a xenon lamp. Spectra were corrected for instrumental response. Solid-state low-temperature measurements were made using a cryogenic sample holder of local design. Powder samples were attached to the holder with a mixture of copper powder, Cryogen oil (used for mounting crystals for X-ray structures), and collodion (an ether- and alcohol-soluble transparent nitrocellulose). The glue was scanned for a baseline subtraction. Liquid nitrogen was used to obtain the 77 K measurements using a cell of local design.

Synthesis of $[Au_2(hpp)_2Cl_2]$, 1. The dinuclear Au(II) species, $[Au_2(hpp)_2Cl_2]$, was synthesized by a modification of the procedure previously published.[9] 1,3,4,6,7,8-hexahydro-2*H*-pyrimido[1,2-*a*]-pyrimidine (H-hpp) (139.0 mg, 1.0 mmol) and sodium hydroxide (40.0 mg, 1.0 mmol) were stirred in a flask with 50.0 mL THF for 3 days to form the sodium salt, Na[hpp]. To the flask, solid (THT)-AuCl (THT = tetrahydrothiophene) (321.0 mg, 1.0 mmol) was added. The solution was stirred in air for 24 h to form a dark green solution after filtering off the NaCl and black residues. The product, $[Au_2(hpp)_2Cl_2]$, formed by hexanes precipitation was filtered and dried under vacuum (200.0 mg, yield 54%). Orange crystals suitable for structural analysis were grown from a THF solution layered with hexanes. ^{1}H NMR ($CDCl_3$, ppm): δ = 1.95 (quin, CH_2), 3.40 (t, CH_2), 3.51 (t, CH_2). UV−vis (1.1×10^{-4} in THF at RT), λ_{max} (nm): ($\epsilon_{L/M-cm}$) 425 (29.9×10^3), 405 (26.7×10^3), 350 (27.3×10^3).

Synthesis of $[Au_4(hpp)_4]$, 2. The above procedure used for the synthesis of $[Au_2(hpp)_2Cl_2]$ was followed for the synthesis of $[Au_4(hpp)_4]$ complex, but ethanol was used as the solvent instead of THF. Ethanol was evaporated off under vacuum and 5 mL THF was added. The solution was filtered to remove the NaCl. A white precipitate was obtained after adding hexanes (240 mg, 72% yield).

(4) Fackler, J. P., Jr. *Inorg. Chem.* **2002**, *41*, 6959−6972 and references cited therein.
(5) Mohamed, A. A.; Abdou, H. E.; Irwin, M. D.; Lopez-de-Luzuriaga, J. M.; Fackler, J. P., Jr. *J. Cluster Sci.* **2004**, *14*, 253−265.
(6) Yan, Z.; Chinta, S.; Mohamed, A. A.; Fackler, J. P., Jr.; Goodman, D. W. *J. Am. Chem. Soc.* **2005**, *127*, 1604−1605.
(7) (a) Barker, J.; Kilner, M. *Coord. Chem. Rev.* **1994**, *133*, 219−300 and references cited therein. (b) Patai, S. *The Chemistry of Amidines and Imidates*; Wiley: New York, 1975; Vol. 1.
(8) (a) Cotton, F. A.; Gruhn, N. E.; Gu, J.; Huang, P.; Lichtenberger, D. L.; Murillo, C. A.; Van Dorn, L. O.; Wilkinson, C. C. *Science* **2002**, *298*, 1971−1974. (b) Wilkinson, C. Ph.D. Thesis, Texas A&M University, 2005. (c) Soria, D. B.; Grundy, J.; Coles, M. P.; Hitchcock, P. B. *J. Organomet. Chem.* **2005**, *690*, 2278−2284. (c) Cotton, F. A.; Durivage, J. C.; Gruhn; Lichtenberger, D. L.; Murillo, C. A.; Van, L. O.; Wilkinson, C. W. *J. Phys. Chem. B* **2006**, *110*, 19793−19798.
(9) Irwin, M. D.; Abdou, H. E.; Mohamed, A. A.; Fackler, J. P., Jr. *Chem. Commun.* **2003**, *23*, 2882−2883.
(10) Abdou, H. E.; Mohamed, A. A.; Fackler, J. P., Jr. *Inorg. Chem.* **2005**, *44*, 166−168.

Colorless crystals suitable for structural analysis were grown from a THF solution layered with hexanes. ^{1}H NMR ($CDCl_3$, ppm): δ = 1.80 (quin, CH_2), 3.62 (t, CH_2), 3.68 (t, CH_2). UV−vis (1.8×10^{-5} in THF at RT); λ_{max} (nm): ($\epsilon_{L/M-cm}$) 425 (14.5×10^3), 405 (13.1×10^3), 370 (12.8×10^3).

Synthesis of $[Au_4(tbo)_4]$, 3. H-tbo (111 mg, 1 mmol) was stirred with (40 mg, 1 mmol) of NaOH in 20 mL of THF (15 mL)/CH_2Cl_2 (5 mL) for 24 h. Au(THT)Cl (320 mg, 1 mmol) was added and stirring continued for additional 3 h. The solution was filtered to remove the NaCl. A white precipitate was obtained after adding hexanes (265 mg, 79% yield). Colorless crystals suitable for structural analysis were grown from a THF solution layered with hexanes.

Synthesis of $[(PhCOO)_2Au_4(hpp)_4Ag_2(PhCOO)_2]$. The dinuclear complex, $[Au_2(hpp)_2Cl_2]$, was reacted with excess silver benzoate in THF/CH_3CN (1:3) mixture. Green crystals formed upon slow evaporation of the solvent mixture. UV−vis: λ_{nm} 575, 440, 303, 273. This product, formed in an attempt to remove the chlorine atoms from $[Au_2(hpp)_2Cl_2]$ and reduce it, was characterized structurally and found to have the arrangement found in Chart 3. It is reported here because it is the result of a reasonable attempt to form a Au(I) product. The structure appears in the Supporting Information. Further studies of this material and other reactions of **1** are under investigation.

Structure Determination. Data were collected using a Siemens (Bruker) SMART CCD (charge-coupled device) based diffractometer equipped with a LT-2 low-temperature apparatus operating at 110 K. A suitable crystal was chosen and mounted on a glass fiber using cryogenic grease. Data were measured using omega scans of 0.3° per frame for 60 s, such that a hemisphere was collected. Cell parameters were retrieved using SMART software and refined using SAINT on all observed reflections.[11] Data reductions were performed using SAINT software.[12] Absorption corrections were applied using SADABS supplied by George Sheldrick.[13] The structure was solved by direct methods using SHELXS-97 and refined by least-squares on F2, with SHELXL-97 incorporated in SHELXTL-PC V 5.03.[14,15] The structures were determined in the space group *Iba*2 and $P\bar{1}$ by analysis of systematic absences. Hydrogen atom positions were calculated by geometrical methods and refined as a riding model.

Results and Discussion

Synthesis and Characterization. The solvent plays an especially important role as to whether a dinuclear Au(II) or a tetranuclear Au(I) species is obtained when Na(hpp) is reacted with (THT)AuCl. In THF the product is the dinuclear Au(II) species, $[Au_2(hpp)_2Cl_2]$, **1**, along with gold metal. In oxidizing solvents such as the chlorocarbon dichloromethane, **1** is produced in high yield without Au(0) formation, Chart 2. If ethanol is used as the solvent, the product is the tetranuclear Au(I) species, $[Au_4(hpp)_4]$. A possible rationalization of the behavior in the two solvents is that ethanol solvates the $[(THT)Au]^+$ reducing its potential[32] for oxidation compared with the (THT)AuCl. Several reducing agents were used in an attempt to reduce the Au(II) complex, including KC_8 or K but each produced gold metal. Using silver carboxylates such as silver benzoate in CH_3CN/THF to remove the chlorides formed a green product with mixed metals and ligands. The gold(II)−silver(I) complex $[(PhCOO)_6Au_4(hpp)_2Ag_2]$, Chart 3, forms with the distances (see Supporting Information) for Au−Au, 2.4473(19) Å, Au−Ag, 3.344(3) Å, and Ag−Ag, 2.771(6) Å.[16]

Chart 2. Synthesis of $[Au_2(hpp)_2Cl_2]$, **1**, and $[Au_4(hpp)_4]$, **2**

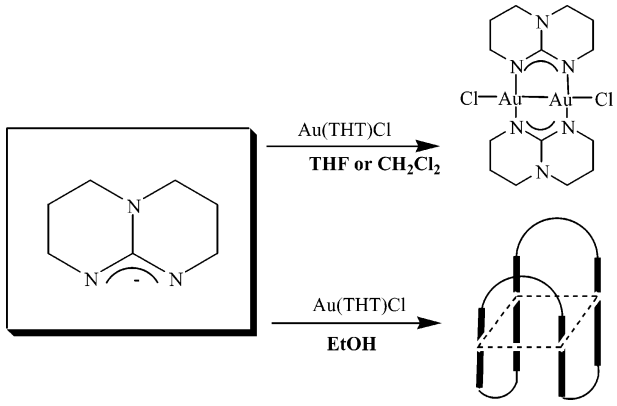

Crystals of $[Au_2(hpp)_2Cl_2]$ were formed readily as dark orange blocks and colorless needles for $[Au_4(hpp)_4]$ and $[Au_4(tbo)_4]$. The dinuclear Au(II) species was analyzed by electrospray mass spectrometry and showed a significant peak at 705 *m*/*e* attributed to the fragment $[Au_2Cl(hpp)_2]^+$. The most significant peak found in the negative ion mass spectrum of the tetranuclear Au(I) species, $[Au_4(hpp)_4]$, is found at 475 *m*/*e*. It can be attributed to the fragment $[Au(hpp)_2]^-$.

The dinuclear, $[Au_2(hpp)_2Cl_2]$, and tetranuclear, $[Au_4(hpp)_4]$, products were analyzed using UV−vis spectroscopy, Figure 1. The UV−vis spectrum of the tetranuclear Au(I) species in THF produced three peaks at around 370, 405, and 425 nm. The UV−vis spectrum of the dinuclear Au(II) species in THF showed three peaks at around 350, 400, and 425 nm. The peak at 425 nm tails off at around 650 nm.

The tetranuclear gold(I) amidinate complexes show a bright green luminescence under UV light, with an emission at around 490 nm and a weak emission at around 570 nm, in the solid state, at room temperature, and 77 K.[5,10] The luminescence of **2** is green under a hand-held UV lamp with a structured emission centered at 470 nm, Figure 1. The average spacing between the maxima is ~1454 cm^{-1}, typical of C═N bonding vibrations. The emission is more structured in **2** than in the tetranuclear Au(I) amidinate and pyrazolate complexes. The emission wavelength in **2** is lower than those of other tetranuclear gold−nitrogen complexes such as $[Au_4(Bu\text{-}pz)_4]$, 541 nm and $[Au_4(4\text{-}Me\text{-}form)_4]$, 500 nm.[3h,5] On the basis of these observations, the emission appears to

(11) SMART V 4.043 Software for the CCD Detector System, Bruker Analytical X-ray Systems, Madison, WI, 1995.
(12) SAINT V 4.035 Software for the CCD Detector System, Bruker Analytical X-ray Systems, Madison, WI, 1995. SAINT V 4.035 Software for the CCD Detector System, Bruker Analytical X-ray Systems, Madison, WI, 1995.
(13) SADABS. *Program for Absorption Corrections Using Siemens CCD Based on the Method of Robert Blessing*, Blessing, R. H. *Acta Crystallogr., Sect. A: Found. Crystallogr.* **1995**, *51*, 33.
(14) Sheldrick, G. M. SHELXS-97, *Program for the Solution of Crystal Structure*, University of Göttingen, Germany, 1997.
(15) SHELXTL 5.03 (PC-Version), *Program Library for Structure Solution and Molecular Graphics*, Bruker Analytical X-ray Systems, Madison, WI, 1995.
(16) Mohamed, A. A.; Fackler, J. P., Jr. Unpublished results.

Chart 3. The Product, $[(PhCOO)_6Au_4(hpp)_2Ag_2]$, from the Reaction of $[Au_2(hpp)_2Cl_2]$ with Silver Benzoate

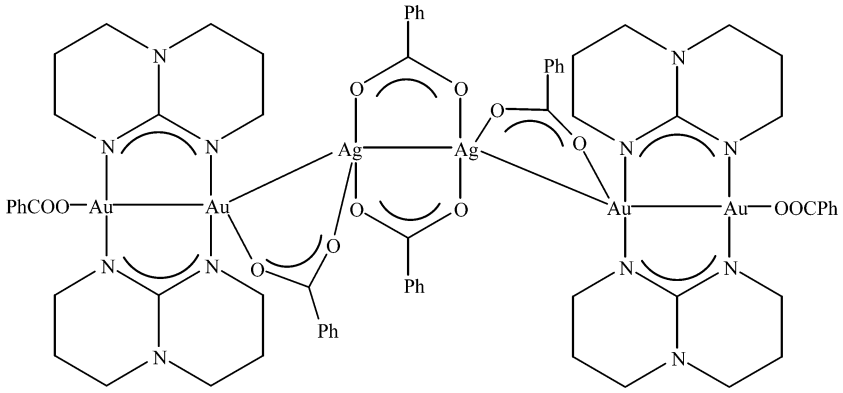

involve ligand-to-metal charge transfer, LMCT, from a π^*-electronic state of the ligand.

Molecular Structures. The X-ray structure of **1** reveals a Au(II)−Au(II) distance of 2.4752(9) Å, Figure 2, which is shorter than the distance observed in $[Au_2(2,6\text{-}Me_2\text{-form})_2\text{-}Cl_2]$ (2.617 Å).[10] This dramatic decrease in distance results from the formation of two Au−Cl bonds and a single Au−Au bond along a common axis, forming a stable d^9-d^9 system.

The molecular structures of $Mo_2(hpp)_4$ and $W_2(hpp)_4$ show M−M distances of 2.067(1) and 2.162(1) Å, respectively.[8] These two complexes contain the shortest Mo_2^{4+} or W_2^{4+} quadruple bonds known. The bicyclic guanidinate ligand, hpp, also stabilizes high oxidation states of various metals.[33]

The tetranuclear complex $[Au_4(hpp)_4]$ crystallizes as colorless crystals in the triclinic space group $P\bar{1}$ with four gold atoms in a parallelogram arrangement, Figure 3. The gold−gold distances range from 2.8975(5)−2.9392(6) Å and are longer than those in the silver complex $[Ag_4(hpp)_4]$, Ag−Ag = 2.8614(6) Å but similar to those in the tetranuclear gold amidinate complexes.[9] The hpp ligands are bridged above and below the near plane of the four Au(I) atoms. The hpp ligand shows a different behavior with different group 11 elements, forming tetranuclear complexes with gold and silver.[9] Only a dinuclear complex of copper(I) has been reported to date.[17]

In the Au(II) complex, the amide C−N bond of the hpp ligand shows double bond character. The amide C(7)−N(2), 1.336(13) Å, is shorter than the CN_2 of the amidine, 1.341-(16) and 1.350(16) Å. The range of Au−N distances in **1** is

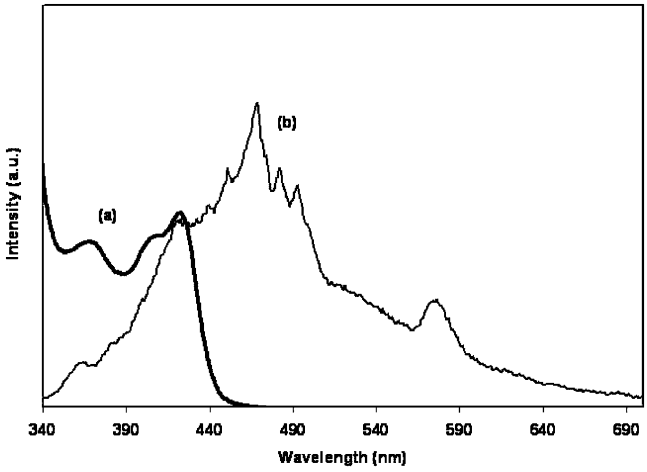

Figure 1. (a) UV−vis spectrum of $[Au_4(hpp)_4]$ (1.8×10^{-5} M) in THF at RT. (b) Emission spectrum of $[Au_4(hpp)_4]$ in the solid state at 77K with the excitation wavelength at 280 nm.

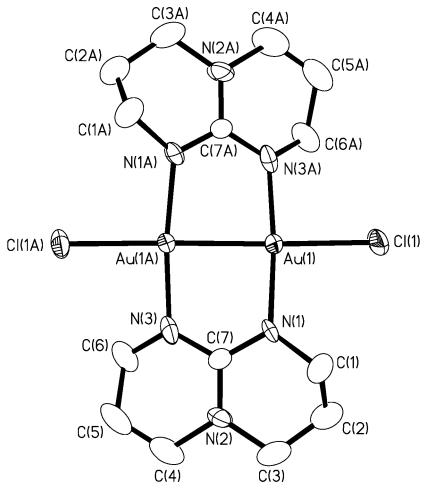

Figure 2. Structure of $[Au_2(hpp)_2Cl_2]$, **1**, at 50% probability. Hydrogen atoms are omitted for clarity. Au−Au = 2.4752(9) and Au−Cl = 2.408(3) Å.

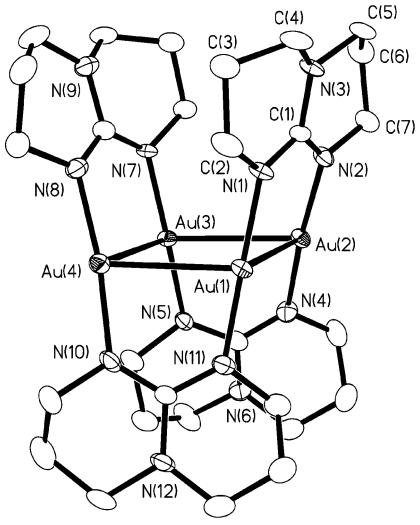

Figure 3. Thermal ellipsoid plot of $[Au_4(hpp)_4]$, **2**, is drawn at the 50% probability level. Hydrogen atoms are omitted for clarity. Au···Au = ~2.92 Å.

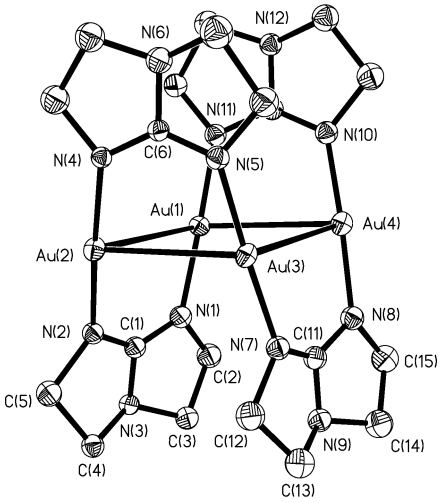

Figure 4. Thermal ellipsoid plot of $[Au_2(tbo)_4]$, **3**, is drawn at the 50% probability level. Hydrogen atoms are removed for clarity. Au···Au = ∼3.18 Å.

2.010(11)−2.062(9) Å, which is similar to the Au−N distance in the dinuclear Au(II) amidinate complex $[Au_2(2,6\text{-}Me_2\text{-form})_2Cl_2]$, 2.020(8) Å. The range of C−N amide distances in **2** is 1.381(8)−1.401(8) Å, which is longer than the C−N amidine bonds of 1.326(8)−1.349(8) Å. The Au(II) atoms are in a square planar arrangement with angles in the range 86.07−94.25° and which add to 359.42°. The N−Au−N angles deviate from linearity, 169.35°. The dihedral angle between the N(1)−Au(1)−N(3A) and N(1A)−Au(1A)−N(3) plane in **1** is 13.3°. The structure is puckered with deviation from the mean plane of 0.35 Å. As discussed below, seven conformations of the rings can be considered. The structure observed appears to the most stable, but the energy differences are small enough to suggest that conformational variability in solution.

The four gold atoms in $[Au_4(tbo)_4]$, **3**, are located at the corner of a rhomboid with the tbo ligands bridged above and below the near plane of the four Au(I) atoms, Figure 4. The NC bond length in the unit of the **3** is ∼1.32 Å, indicating delocalization across the NCN bridge. The average Au···Au distance is 3.16 Å. The angles at Au···Au···Au are acute 66.03(3)−66.12(3)° and obtuse 111.92.64(3)−115.82(3)°.

Computational Methods. Full geometry optimizations were performed on the experimental compounds $[Au_2(hpp)_2Cl_2]$, **1**, $[Au_4(hpp)_4]$, **2**, and the theoretical model $[Au_2(hpp)_2]$. All calculations were performed with the Gaussian 03 (G03) suite of programs[18] using either BSI (correlation consistent polarized valence double-ζ basis set (cc-pVDZ)[19] for C, N, and H and a triple-ζ basis set with an effective core potential (ECP)[20] for the Au atoms) or BSII (BSI with the addition of an f polarization function on the Au atoms with an exponent[21] of 1.050). Geometry optimizations were performed using density functional theory (DFT)[22] with the MPW1PW91 (Barone's Modified Perdew−Wang 1991 exchange functional and Perdew and Wang's 1991 correlation functional)[23] on all models. To test the consistency of various functionals, selected models were also optimized with the B3LYP (Becke three-parameter hybrid exchange functional[24] and the Lee−Yang−Parr correlation functional)[25] and/or B3PW91 (Becke three-parameter hybrid exchange functional[24] and Perdew and Wang's 1991 correlation functional[26]) functionals. Second-order Møller−Plesset Perturbation theory (MP2)[27] optimizations were also performed on compounds $[Au_2(hpp)_2Cl_2]$, **1**, and the theoretical model $[Au_2(hpp)_2]$ since it is well-known that DFT methods underestimate dispersion forces which are important in Au−Au complexes and normally are better represented at the MP2 or higher *ab intio* level of theory.[28] An MP2 optimization was not performed on $[Au_4(hpp)_4]$, **2**, because it would be prohibitively expensive given the size of this system.

A complete study of the seven conformations available for the hpp ligand in $[Au_2(hpp)_2Cl_2]$, **1**, were performed at the MPW1PW91, B3PW91, and B3LYP levels. It was found that the crystal structure conformation was the lowest energy conformation of the hpp and was lower in energy by a minimum of 1.5 kcal mol^{-1} than any other conformation for all three methods. The Au−Au distance varied by 0.01 Å or less for all conformations and DFT levels of theory. The lowest energy optimized structural parameters are in good agreement with the crystal structure parameters (Figure 5). The optimized Au−Au distance was calculated to be 2.53, 2.54, and 2.56 Å for MPW1PW91, B3PW91, and B3LYP, respectively. All three methods are reasonably close to the crystal structure Au−Au distance of 2.48 Å with MPW1PW91 giving the best value. For all methods, the addition of an f function (BSII) on the gold atoms decreased the Au−Au bond distance by 0.02 Å, bringing the MPW1PW91/ BSII

(17) Cotton, F. A.; Feng, X.; Timmons, D. J. *Inorg. Chem.* **1998**, *37*, 4066−4069.

(18) Gaussian 03, Revision C.02, Frisch, M. J.; Trucks, G. W.; Schlegel, H. B.; Scuseria, G. E.; Robb, M. A.; Cheeseman, J. R.; Montgomery, J. A., Jr.; Vreven, T.; Kudin, K. N.; Burant, J. C.; Millam, J. M.; Iyengar, S. S.; Tomasi, J.; Barone, V.; Mennucci, B.; Cossi, M.; Scalmani, G.; Rega, N.; Petersson, G. A.; Nakatsuji, H.; Hada, M.; Ehara, M.; Toyota, K.; Fukuda, R.; Hasegawa, J.; Ishida, M.; Nakajima, T.; Honda, Y.; Kitao, O.; Nakai, H.; Klene, M.; Li, X.; Knox, J. E.; Hratchian, H. P.; Cross, J. B.; Bakken, V.; Adamo, C.; Jaramillo, J.; Gomperts, R.; Stratmann, R. E.; Yazyev, O.; Austin, A. J.; Cammi, R.; Pomelli, C.; Ochterski, J. W.; Ayala, P. Y.; Morokuma, K.; Voth, G. A.; Salvador, P.; Dannenberg, J. J.; Zakrzewski, V. G.; Dapprich, S.; Daniels, A. D.; Strain, M. C.; Farkas, O.; Malick, D. K.; Rabuck, A. D.; Raghavachari, K.; Foresman, J. B.; Ortiz, J. V.; Cui, Q.; Baboul, A. G.; Clifford, S.; Cioslowski, J.; Stefanov, B. B.; Liu, G.; Liashenko, A.; Piskorz, P.; Komaromi, I.; Martin, R. L.; Fox, D. J.; Keith, T.; Al-Laham, M. A.; Peng, C. Y.; Nanayakkara, A.; Challacombe, M.; Gill, P. M. W.; Johnson, B.; Chen, W.; Wong, M. W.; Gonzalez, C.; Pople, J. A.; Gaussian, Inc., Wallingford, CT, 2004.

(19) Dunning, T. H., Jr. *J. Chem. Phys.* **1989**, *90*, 1007.

(20) Schwerdtfeger, P.; Dolg, M.; Schwarz, W. H. E.; Bowmaker, G. A.; Boyd, P. D. W. *J. Chem. Phys.* **1989**, *91*, 1762.

(21) Ehlers, A. W.; Böhme, M.; Dapprich, S.; Gobbi, A.; Höllwarth, A.; Jonas, V.; Köhler, K. F.; Stegmann, R.; Veldkamp, A.; Frenking, G. *Chem. Phys. Lett.* **1993**, *208*, 111.

(22) Parr, R. G.; Yang, W. *Density-Functional Theory of Atoms and Molecules*; Oxford University Press: Oxford, 1989.

(23) Adamo, C.; Barone, V. *J. Chem. Phys.* **1998**, *108*, 664.

(24) Becke, A. *J. Chem. Phys.* **1993**, *98*, 5648.

(25) Lee, C.; Yang, W.; Parr, R. G. *Phys. Rev.* **1988**, *37*, 785.

(26) (a) Perdew, J. P. *Electronic Stucture of Solids '91*; Akademie Verlag: Berlin, 1991; p 11. (b) Perdew, J. P.; Chevary, S. H.; Vosko, S. H.; Jackson, K. A.; Pederson, D. J.; Singh, D. J.; Foilhais, C. *Phys. Rev. B* **1992**, *46*, 6671; **1993**, *48*, 4978(E).

(27) Møller, C.; Plesset, M. S. *Phys. Rev.* **1934**, *46*, 618.

(28) Pyykkö, P. *Chem. Rev.* **1997**, *97*, 597.

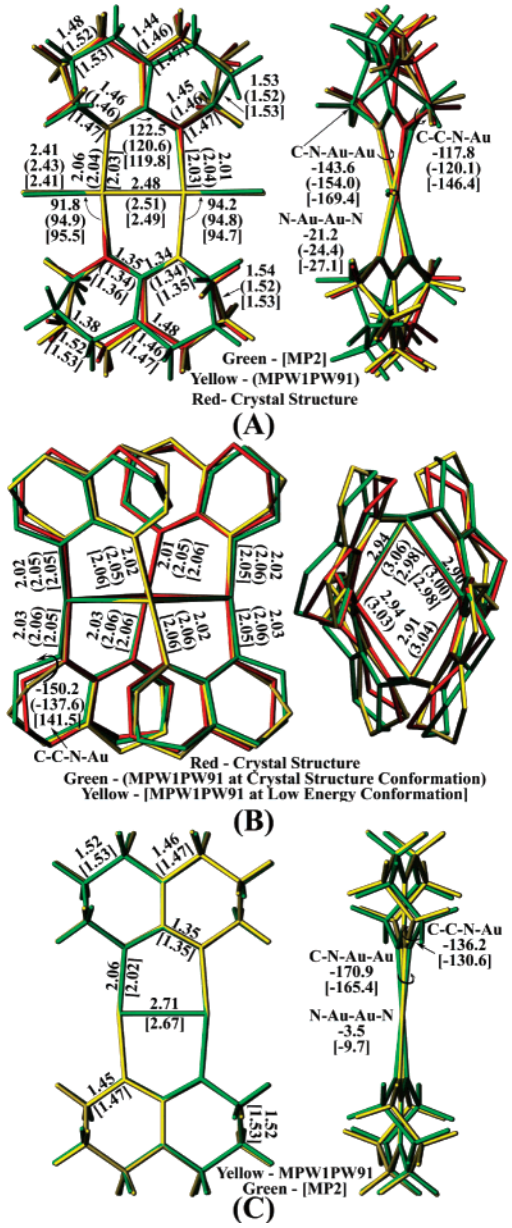

Figure 5. (a) Overlay of the crystal structure, MP2/BSII, and MPW1PW91/BSII optimized structures for $[Au_2Cl_2(hpp)_2]$, **1**. (b) Overlay of the crystal structure and **2** conformation (**2a** and **2b**) optimized at the MPW1PW91/BSII level of theory for $[Au_4(hpp)_4]$. (c) Overlay of the MPW1PW91/BSII and MP2/BSII optimized structure for the theoretical model $[Au_2(hpp)_2]$.

Au−Au bond distance to 2.51 Å and within 0.03 Å of the experimental value. MP2 optimizations were also performed on the three lowest energy conformers of **1** and were found to have similar energetic and structural parameters as the DFT results. The Au−Au distance at the MP2 level of theory with BSI for the lowest energy conformer of **1** is 2.55 Å. At the MP2 level of theory, the addition of an f function (BSII) shortened the Au−Au distance by 0.06 Å, which is a much larger effect than that at the DFT level (0.02 Å) to give a Au−Au bond distance of 2.49 Å, which is within 0.01 Å of the experimental value (Figure 5).

Molecular orbital analyses using the SCPA method[29] implemented in AOMIX[30] (Table 5) for the most favorable conformation of **1** and $[Au_2(hpp)_2]$ using BSII at the MPW1PW91 and MP2 levels of theory were performed. For

Table 1. Crystallographic Data for $[Au_2(hpp)_2Cl_2]$, **1**, $[Au_4(hpp)_4]$, **2**, and $[Au_4(tbo)_4]$, **3**

	1	**2**	**3**
formula	$C_{14}H_{24}Au_2Cl_2N_6$	$C_{28}H_{48}Au_4N_{12}$	$C_{20}H_{36}Au_4N_{12}$
fw	741.22	1340.25	1232
cryst syst	orthorhombic	triclinic	triclinic
space group	*Iba*2	*P*	*P*
a (Å)	10.866(5)	8.5960(15)	11.476(3)
b (Å)	20.745(5)	11.802(2)	15.033(4)
c (Å)	8.164(5)	16.789(3)	17.185(5)
α (deg)	90	88.035(3)	112.028(5)
β (deg)	90	86.872(3)	105.673(5)
γ (deg)	90	73.684(3)	91.165(5)
V (Å^3)	1840.3(15)	1631.9(5)	2621.5(13)
Z	4	2	4
GOF	1.043	1.064	0.7107
R1, wR2	0.0365, 0.0903	0.0335, 0.0809	0.0707, 0.2801

Table 2. Selected Bond Distances (Å) and Angles (deg) for $[Au_2(hpp)_2Cl_2]$, **1**

bond distances (Å)			
	2.4752(9)	Au(1)−N(3A)	2.010(11)
Au(1)−N(1)	2.062(9)	Au(1)−Cl(1)	2.408(3)
N(1)−C(7)	1.341(16)	N(3)−C(7)	1.350(16)
N(2)−C(7)	1.336(13)		
bond angles (deg)			
N(3A)−Au(1)−N(1)	169.4(6)	N(1)−Au(1)−Cl(1)	94.2(3)
N(1)−C(7)−N(3)	122.5(10)	N(3)−Au(1A)−Cl(1A)	91.9(3)

Table 3. Selected Bond Distances (Å) and Angles (deg) for $[Au_4(hpp)_4]$, **2**

bond distances (Å)			
Au(1)−Au(2)	2.8975(5)	Au(1)−Au(4)	2.9130(6)
Au(2)−Au(3)	2.9392(6)	Au(3)−Au(4)	2.9365(5)
Au(1)−N(11)	2.013(6)	Au(4)−N(8)	2.030(6)
C(1)−N(2)	1.326(8)	C(1)−N(1)	1.349(8)
C(1)−N(3)	1.391(8)		
bond angles (deg)			
Au(2)−Au(1)−Au(4)	113.720(11)	Au(1)−Au(2)−Au(3)	67.275(10)
Au(1)−Au(4)−Au(3)	67.112(10)	Au(4)−Au(3)−Au(2)	111.794(11)
N(11)−Au(1)−N(1)	175.4(2)	N(10)−Au(4)−N8	172.2(2)
N(4)−Au(2)−N(2)	172.8(2)	N(7)−Au(3)−N(5)	174.4(2)
N(2)−C(1)−N(1)	121.0(6)	N(5)−C(8)−N(4)	123.0(6)

Table 4. Selected Bond Distances (Å) and Angles (deg) for $[Au_4(tbo)_4]$, **3**

bond distances (Å)			
Au(1)−N(1)	2.039(16)	N(2)−C(1)	1.32(3)
Au(1)−Au(2)	3.1139(12)	Au(3)−Au(4)	3.1889(12)
Au(1)−Au(4)	3.1563(13)	Au(3)−Au(2)	3.2220(13)
bond angles (deg)			
Au(1)−Au(2)−Au(3)	66.12(3)	N(1)−C(1)−N(2)	131.1(18)
Au(4)−Au(3)−Au(2)	111.92(3)	N(1)−C(1)−N(3)	112.9(18)
Au(1)−Au(4)−Au(3)	66.03(3)	N(2)−C(1)−N(3)	115.9(17)
Au(2)−Au(1)−Au(4)	115.82(3)	N(7)−Au(3)−N(5)	177.7(7)

1 at the MPW1PW91 level, the HOMO through HOMO-3 are mainly hpp-based orbitals (72% or higher, Figure 6) whereas at the MP2 level of theory there is significantly more gold and chlorine character in the HOMO and HOMO-2, but the HOMO-1 and HOMO-3 are very similar to the MPW1PW91 results (Table 5). At both the MPW1PW91 and MP2 levels of theory the LUMO has approximately 50% gold $d_{x^2-y^2}$ character (48% and 57%, respectively), 25% hpp (28% and 23%, respectively), and 25% chlorine (25% and 20%, respectively). These results are consistent with the observed UV−vis spectra having a number of moderately weak low-energy excitations that involve orbitals that have

Table 5. Molecular Orbital Compositions for $[Au_2Cl_2(hpp)_2]$, **1**, $[Au_4(hpp)_4]$, **2**, and $[Au_2(hpp)_2]$

	energy (eV)		gold		chlorine		hpp	
$[Au_2Cl_2(hpp)_2]$	MP2	MPW1PW9 1	MP2	MPW1PW 91	MP2	MPW1PW 91	MP2	MPW1PW 91
LUMO	0.10	−3.17	57	48	20	25	23	28
HOMO	−8.72	−5.98	36	21	25	7	39	72
HOMO-1	−9.80	−6.56	7	5	8	5	86	90
HOMO-2	−9.85	−6.78	24	7	31	0	45	93
HOMO-3	−10.15	−6.96	6	9	2	10	92	81
$[Au_4(hpp)_4]^a$	**2a**	**2b**	**2a**	**2b**	**2a**	**2b**	**2a**	**2b**
LUMO	−0.15	−0.15	85	85			15	15
HOMO	−4.58	−4.71	20	78			80	22
HOMO-1	−5.07	−4.89	81	20			19	80
HOMO-2	−5.08	−5.05	45	28			55	72
HOMO-3	−5.23	−5.19	36	48			64	52
$[Au_2(hpp)_2]$	MP2	MPW1PW91	MP2	MPW1PW91	MP2	MPW1PW91	MP2	MPW1PW91
LUMO	0.49	−0.15	100	73			0	27
HOMO	−7.39	−4.89	89	19			11	81
HOMO-1	−7.67	−5.19	18	91			82	9
HOMO-2	−8.75	−5.86	5	15			95	85
HOMO-2	−8.94	−5.89	14	5			86	95

[a] MPW1PW91/BSII results.

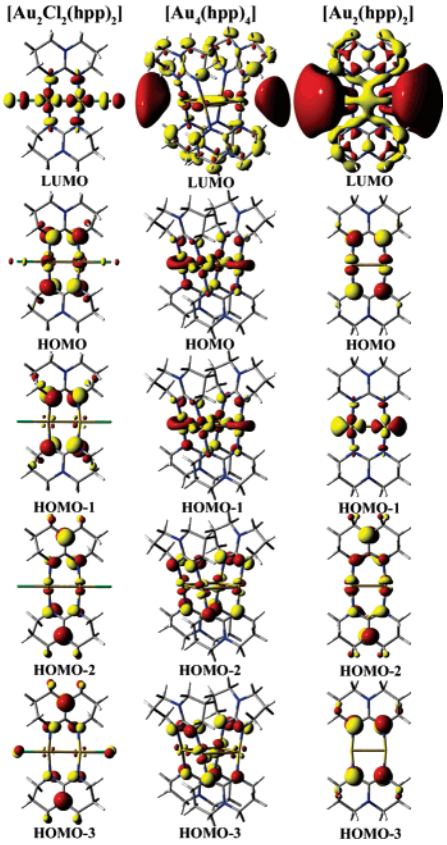

Figure 6. Pictures of the 0.05 contour surface diagram at the MPW1PW91/BSII level for the HOMO-3 through the LUMO of $[Au_2(hpp)_2Cl_2]$ (**1**) and HOMO-3 through the HOMO of $[Au_4(hpp)_4]$ (**2b**), and the theoretical model, $[Au_2(hpp)_2]$. The 0.01 contour surface diagram at the MPW1PW91/BSII of the LUMO for **2b** and $[Au_2(hpp)_2]$ is pictured instead of a value of 0.05 due to large gold s orbital contribution.

strong hpp character. The calculated frontier orbital energy separations are larger than the experimental UV−vis data since relaxation energies are not included in the theoretical results.

Geometry optimizations at the MPW1PW91/BSII level of theory were performed for **2** since the MPW1PW91 functional produced the best structural results for **1**, and it would be prohibitively expensive to perform an MP2 optimization. Two conformations of the hpp ligand were investigated: (a) the crystal structure conformation (**2a**) and (b) a conformation based on the lowest energy conformation for **1** (**2b**). Both conformations were close in energy with a ΔH^o of 2.05 kcal mol^{-1} and $\Delta G°$ of 0.87 kcal mol^{-1} with **2b** lower in energy. The Au−Au bond distances were calculated to be 2.98 Å for **2b**, and 3.00, 3.04, 3.03, and 3.06 Å (average Au−Au distance 3.03 Å) for **2a** within reason to the experimental Au−Au distances of 2.90, 2.91, 2.94, and 2.94 Å (average Au−Au distance 2.92 Å) (Figure 5). A molecular orbital analyses using the SCPA method[29] implemented in AOMIX[29] (Table 5) for **2a** and **2b** were performed and found to be very similar. For **2a** and **2b**, the LUMO has 85% gold s character and 15% ligand character (Figure 6). The HOMOs differ slightly in contributions between **2a** and **2b**. The HOMO in **2a** has mostly ligand character (80%), and the HOMO-1 is mostly gold character (81%) whereas in **2b** these orbitals are switched with the HOMO having mostly gold character (78%) and the HOMO-1 having mostly ligand character (80%). The HOMO-2 and HOMO-3 in **2a** are a mixture of gold and ligand character with the HOMO-2 having 45% gold characters and the HOMO-3 having 36% gold characters. The HOMO-2 and HOMO-3 in **2b** are also a mixture of gold and ligand character with the HOMO-2 having 28% gold character and the HOMO-3 having 48% gold character. These results are also consistent with the UV−vis spectra for **2**.

The thermodynamics for the reduction of **1** to $[Au_2(hpp)_2]$ and $Cl_2(g)$ was calculated using BSII at the MPW1PW91, B3PW91, B3LYP, and MP2[31] levels of theory. It was

(29) Ros, P.; Schuit, G. C. A. *Theor. Chim. Acta* **1966**, *4*, 1.

(30) (a) Gorelsky, S. I. AOMix program, http://www.sg-chem.net/. (b) Gorelsky, S. I.; Lever, A. B. P. *J. Organomet. Chem.* **2001**, *635*, 187−196.

(31) Thermal parameters were taken from the mpw1pw91 calculations.

calculated that this is an endothermic reaction with a $\Delta H°$ of 50.0, 48.6, 45.8, and 69.5 kcal mol^{-1} and a $\Delta G°$ of 38.3, 37.5, 35.3, and 57.8 kcal mol^{-1}, respectively. The fact that the reaction is thermodynamically unfavorable is consistent with the difficulty in experimentally obtaining the compound $[Au_2(hpp)_2]$. The $\Delta H°$ ($\Delta G°$) for the reduction of **1** to **2a** and **1** to **2b** were also calculated using BSII at the MPW1PW91 level of theory and found to be exothermic by 83.6 kcal mol^{-1} (74.7 kcal mol^{-1}) and 85.7 kcal mol^{-1} (75.6 kcal mol^{-1}), respectively.

Conclusions

The synthesis of gold−guanidinate-like complexes is solvent dependent. The reaction of (THT)AuCl and Na(hpp) in THF or halogenated solvents produces the dinuclear Au(II) complex, $[Au_2(hpp)_2Cl_2]$, **1**, however, the reaction in ethanol produces the tetranuclear gold(I) complex, $[Au_4(hpp)_4]$, **2**. In the gold hpp complex **1**, the HOMO is mostly ligand based with a small Au−Au δ^* contribution, and the LUMO is a mixture of approximately 50% Au−Au σ^* ($d_{x^2-y^2}$), 25% chlorine p_y, and 25% hpp. In the gold hpp complex **2**, the HOMO and HOMO-1 have a mixture of gold $d_{z^2-y^2}/d_{z^2}$ and ligand character and the LUMO has 85% Au−Au σ^* (s) character and 15% ligand character. The LUMO in **2** does not have Au−Au σ-bonding character as previously found for other dinuclear Au(I) complexes.

Acknowledgment. The Robert A. Welch Foundation, Houston, TX, is acknowledged for financial support. A.P.M. acknowledges NSF-REU program for financial support during the summer of 2005 at Texas A&M University. The Super Computing Facility and Laboratory for Molecular Simulation at Texas A&M University are acknowledged for providing computer time and software. Htbo was a generous gift from Cotton Laboratory.

Supporting Information Available: The .cif files of complexes **1**−**3**. This material is available free of charge via the Internet at http://pubs.acs.org.

IC701399S

(32) Latimer, W. M. *Oxidation Potentials*; Prentice Hall: Upper Saddle River, NJ, 1952.

(33) Cotton[8] has discussed the ability of the hpp ligand to stabilize high oxidation states and relates this property to the delocalizing of electron density over the guanidinate core with the δ orbitals of the metal centers. It is interesting that a structurally similar π delocalized unit exists in dithiocarbamate complexes which also stabilize high oxidation state metal ions[34] and support the oxidation of dinuclear Au(I) complexes to metal−metal-bonded Au(II) species.[35]

(34) Fackler, J. P., Jr.; Avdeef, A.; Fischer, R. G., Jr. *J. Am. Chem. Soc.* **1973**, *95*, 774.

(35) Calabro, D. C.; Harrison, B. A.; Palmer, G. T.; Moguel, M. K.; Rebbert, R. L.; Burmeister, J. L. *Inorg. Chem.* **1981**, *20*, 4311.